Environment International 195 (2025) 109255

Contents lists available at ScienceDirect

Environment International

journal homepage: www.elsevier.com/locate/envint

Full length article

Exploring seasonal dynamics of sea spray aerosol bioactivity: Insights into molecular effects on human bronchial epithelial cells

Zixia Liu [a], Emmanuel Van Acker [b], Maarten De Rijcke [c], Filip Van Nieuwerburgh [d], Colin Janssen [a,b], Jana Asselman [a,*]

[a] Blue Growth Research Lab, Ghent University, Wetenschapspark 1, Bluebridge, 8400 Oostende, Belgium
[b] GhEnToxLab, Ghent University, Coupure Links 653, 9000 Ghent, Belgium
[c] Flanders Marine Institute (VLIZ), Research Division, Ocean and Human Health, InnovOcean Campus, Jacobsenstraat 1, 8400 Oostende, Belgium
[d] Laboratory of Pharmaceutical Biotechnology, Ghent University, Ottergemsesteenweg 460, 9000 Ghent, Belgium

ARTICLE INFO

Keywords:
sea spray aerosol (SSA)
Bronchial epithelial cells
RNA sequencing
Biogenics hypothesis
mTOR pathway
Seasonal variation
Oceans and human health

ABSTRACT

Sea spray aerosol (SSA) is a complex mixture of natural substances that can be inhaled by coastal residents. Previous studies have suggested that SSA may have positive effects on human health, but the molecular mechanisms and the factors influencing these effects are poorly understood. In this study, we exposed human bronchial epithelial cells (BEAS-2B) to natural SSA samples, collected monthly using quartz microfiber filters mounted on tripods within 15 m of the waterline, with air drawn through pumps, throughout a one-year period at the Ostend coast, Belgium, and measured cellular gene expression changes using RNA sequencing. To simulate environmentally relevant exposure conditions, SSA extracts were applied at scaled doses equivalent to human alveolar exposure levels (multiplicative factors M = 10, 20, 40, and 80). We found that SSA exposure influenced the expression of genes involved in critical signaling pathways: mTOR, PI3K, Akt, and NF-κB were down-regulated, while AMPK was upregulated. Downregulation of mTOR, PI3K, Akt, and NF-κB potentially indicates a protective response against tumor-promoting and inflammatory signals, whereas upregulation of AMPK may confer a beneficial effect on metabolic regulation. The number and direction of differentially expressed genes (DEGs) varied depending on the SSA sampling time and correlated with the phytoplankton density and chemical diversity of the SSA samples. Our results suggest that SSA contains bioactive compounds that may originate from marine algae and modulate cellular processes related to human health. We provide novel insights into the molecular effects of SSA exposure and highlight its potential as a source of natural therapeutics. To our knowledge, this is the first study to expose human lung cells to natural SSA at environmentally relevant levels, presenting a pioneering exploration of seasonal variations in exposure effects.

1. Introduction

The coastal environment, an important element of "blue spaces," is increasingly recognized not only for its psychological benefits but also for its potential physiological impacts on human health (Bell et al., 2015; Gascon et al., 2017; Wheeler et al., 2012). Beyond the well-documented restorative effects on mental well-being (Gascon et al., 2015; White et al., 2021), recent research suggests that aerosolized biogenic compounds present in sea spray aerosols (SSAs) might play a significant role in influencing human health (Moore, 2015). These compounds, which include a variety of bioactive substances, are hypothesized to interact with cellular signaling pathways such as mTOR, Akt, or PI3K (Asselman et al., 2019; Moore, 2015; van Acker et al., 2020). This interaction could have both positive and negative health implications for individuals residing in coastal areas. Such a perspective expands the traditional understanding of the health benefits associated with coastal environments, moving beyond psychological effects to encompass a potential biochemical impact.

The major transport route of marine biogenics is via SSA (Lang-Yona et al., 2014), primarily generated by the bursting of bubbles take place in the sea surface microlayer (SSML) (Keene et al., 2007). The SSML, a unique interface between the air and ocean, is rich in various hydrophobic and amphiphilic substances, including biogenic compounds (Aller et al., 2005). These compounds are often found in much higher

* Corresponding author.
E-mail address: jana.asselman@ugent.be (J. Asselman).

https://doi.org/10.1016/j.envint.2025.109255
Received 15 October 2024; Received in revised form 2 January 2025; Accepted 2 January 2025
Available online 4 January 2025

concentrations in SSAs compared to bulk seawater (Van Acker et al., 2021b), highlighting the significance of SSAs as a carrier for these substances.

Among the diverse sources of marine biogenics, phytoplankton stand out due to their substantial biomass (Bar-On and Milo, 2019) and the wide array of bioactive compounds they release into the ocean. These biogenic compounds, encompassing polysaccharides, lipids, amino acids, and enzymes (Menaa et al., 2021), not only play a crucial role in the marine ecosystem but also have the potential to impact human health when aerosolized, either in positive or negative ways. Several studies have reported the negative health effects of aerosolized marine biogenic compounds during harmful algal blooms (HABs) (Backer et al., 2005; Cheng et al., 2010; Fleming et al., 2009). The phycotoxins produced during HABs were confirmed to be aerosolized and exist in SSAs of coastal regions (Fleming et al., 2005), and the relationship between respiratory symptoms of people living in coastal regions after HAB events has been quantified by an epidemiological study (Hoagland et al., 2009). Notably, due to their hydrophobic nature, some phycotoxins were reported to be enriched up to thousands of times in SSAs (Van Acker et al., 2021b), intensifying their potential impact. Beyond HAB events, a recent study has shown that a biogenic compound produced by marine algae can be detected in coastal air, even at ambient algal concentrations (Van Acker et al., 2021a). This indicates the coastal residents may be continuously exposed to marine biogenic compounds throughout the year, suggesting a broader potential health impact of SSAs on coastal populations.

Furthermore, certain marine algal compounds have demonstrated anti-cancer or anti-inflammatory properties, which are studied for their pharmaceutical and cosmeceutical applications (Alves et al., 2018; Dong et al., 2020; Pereira, 2018). While characterization of SSA composition has mainly focused on inorganic fractions (Bertram et al., 2018), some biogenic compounds have already been identified (Ault et al., 2013; Bertram et al., 2018; Cochran et al., 2017; DeMott et al., 2016; Miyazaki et al., 2020). The biogenic compound dipalmitoylphosphatidylcholine (DPPC), likely produced by marine algae, has been detected in SSA samples (Van Acker et al., 2021a). Given DPPC is also the main constituent of pulmonary surfactants and has been used as an inhalable surfactant and inhalation enhancer (Hidalgo et al., 2015). As such, DPPC in SSA may have implications for respiratory health. At the molecular level, artificial SSA produced from media containing the phycotoxin homoyessotoxin, as well as natural SSA samples, have been shown to interact with the mTOR pathway at both gene and pathway levels (Asselman et al., 2019).

The studies mentioned above lead us to this expanded biogenics hypothesis: marine algae can release bioactive compounds that get enriched in the SSA; to which coastal residents are continuously exposed. From the exposure side, the detection of marine toxins and other biogenic compounds in SSA (Cheng et al., 2010; Fleming et al., 2009; Van Acker et al., 2021a, 2021b) provides direct evidence that these substances can become airborne and potentially inhaled by people living near the coast. Daily respiratory exposure to SSA may inhibit signaling pathways such as mTOR, Akt or PI3K and thereby positively influence human health. Studies that exposed human cell lines to coastal air (Asselman et al., 2019) or aerosolized marine toxins (van Acker et al., 2020) have supported this hypothesis from the effect side. Each piece of the knowledge puzzle is supported by one or more studies, yet no single study has verified the entire story at an environmentally relevant dose, particularly with regards to the seasonal variation in the production and composition of the SSAs, given the well-recognized variations of phytoplankton composition across seasons.

In this study, we exposed human bronchial epithelial cells (BEAS-2B) to nine natural SSA samples collected at the Belgian coast throughout a one-year campaign. The SSA samples were collected during conditions with strong winds capable of generating white-cap waves, with the wind blowing from the sea to the coast, ensuring the aerosols were primarily composed of SSA. Additionally, we included ambient coastal aerosol samples (AMB, collected during conditions of little wind, ensuring no locally generated SSA was present in the sample), city aerosol samples (CTY), positive controls (POS, mTOR inhibitor PP242), and negative controls (NEG) in the exposure experiments, with each serving as a treatment group. The RNA expressions of each BEAS-2B cell line sample were quantified, compared across treatments, and fitted against environmental factors and the chemical diversity found within the SSA to support the biogenics hypothesis at the molecular level using environmentally realistic conditions.

2. Results

Across all treatment groups, we quantified the expressions of 58,233 genes and 199,234 transcripts. Hierarchical clustering (Fig. 1a) displayed no obvious outliers, suggesting consistent sample quality. A distinct clustering pattern emerged when we applied a cut-off at a height of 40,000 on the dendrogram. This division led to three major clusters (as indicated in SI.11): Cluster 1 comprising samples exposed to SSA during temperate conditions (air temperature 8.39℃ – 16.12℃), Cluster 2 with control samples and those exposed to SSA in cold weather, and Cluster 3 containing samples from hot weather SSA exposures. Intriguingly, SSA collected in cold weather exhibited significantly lower Na^+ content compared to other conditions. A correlation with phytoplankton density (see **Discussions** for details), was noted.

2.1. Differential gene expression in response to treatments

Out of the all genes and transcripts analyzed, 19,768 protein-coding genes and 79,757 transcripts were further examined. Genome DEGs reflect changes at the gene level, while transcriptome DEGs capture specific transcript variants. Analyzing both provides a comprehensive view of cellular responses. Comparing the expression levels of these genes between the NEG group and all the other treatment groups, the SSA group has (one of) the highest number of DEGs across all treatment groups: 91 genome DEGs and 425 transcriptome DEGs at a False Discovery Rate (FDR) <= 0.05, and 32 genome DEGs and 327 transcriptome DEGs at FDR <= 0.01, with a > 2-fold change. Notably, most DEGs were downregulated, except for the positive control group, which showed a higher count of upregulated DEGs. Although the numbers of transcriptome DEGs are generally higher than genome DEGs, the patterns of DEG numbers for each treatment group are comparable. To find as many DEGs as possible that respond to SSA exposure, an FDR <= 0.05 threshold was adopted. Fig. 1b & c illustrate the DEG counts and distributions (volcano plots) for each group. Disregarding the gene type of genome or transcriptome, the AMB, CTY, and SSA treatment groups showed similar patterns in volcano plots, but the dots in the similar position do not necessarily mean the same gene. There are 44 genome DEGs and 106 transcriptome DEGs in the SSA exposure group which are unique; 8 genome DEGs and 61 transcriptome DEGs are shared by the SSA group and POS group. To be noted, there are 27 genome DEGs and 206 transcriptome DEGs shared by the SSA group and the AMB group, which count for 29.7 % and 61.2 % of the SSA group's DEG number. This indicates the ambient coast air may also contain some bioactive compounds as in SSA. There are also some DEGs shared by the SSA group and CTY group, which may be the effects of exposure to city air and were addressed in the **Discussions**. The numbers of shared and unique DEGs across all treatments were visualized in Fig. 1d.

2.2. Genes in mTOR pathway in response to SSA exposure

The mTOR pathway has been reported to be regulated by SSA exposure. To verify this, we compared the expression of these genes across all samples. In the heatmap of the mTOR signal pathway (Fig. 2a), there are two clusters of samples that showed a clear difference in gene expression, which were either in the "temperate" or "hot" weather group. This cluster is composed of 64 samples, among which 48 were in

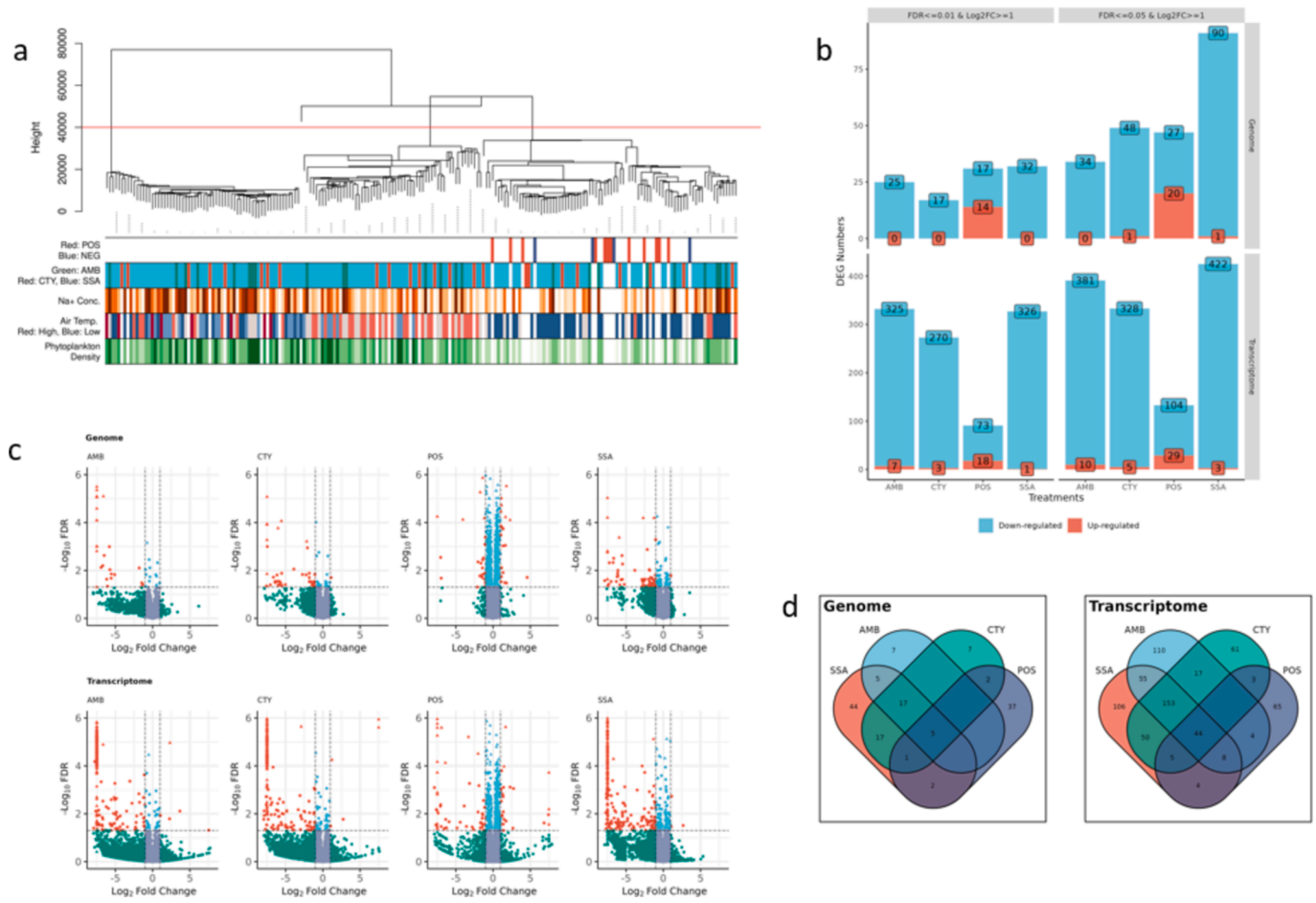

Fig. 1. Differential gene expression in response to treatments. **(a)** Hierarchical clustering of gene expression in samples exposed to SSA under varying environmental conditions. The clustering of gene expression was performed using genome-wide expression profiles and employed the centroid linkage method. Clusters are demarcated by a 40,000 height threshold (red line), with sample leaves colored by treatment: positive or negative control (POS/NEG), ambient air (AMB), city air (CTY), and SSA. Below the dendrogram, metadata corresponding to SSA collection parameters (Na^+ concentration, air temperature, and phytoplankton density) are represented by colors. These colors were assigned based on k-means clustering of the respective metadata values: Na^+ concentration (9 clusters, orange gradient), air temperature (5 clusters, red-blue diverging palette), and phytoplankton density (5 clusters, green gradient). White represents missing values for metadata. **(b)** Counts of genome and transcriptome DEGs categorized by downregulation (blue) and upregulation (red) across treatments. DEGs are identified using thresholds of FDR $\leq$ 0.05 and $|\log2FC| \geq 1$ (right panels) or stricter thresholds of FDR $\leq$ 0.01 and $|\log2FC| \geq 1$ (left panels). **(c)** Volcano plots illustrating the log2 fold change against the negative log10 FDR for DEGs in genome (up) and transcriptome (down) analyses. Genes meeting both thresholds of FDR $\leq$ 0.05 and $|\log2FC| \geq 1$ are highlighted in red, genes meeting only the FDR threshold are shown in blue, and genes meeting only the log2FC threshold are shown in green. Genes not meeting either threshold are depicted in gray. Dashed lines indicate the significance thresholds. **(d)** Venn diagrams representing the overlap and uniqueness of differentially expressed genes (left) and transcripts (right) across four treatment groups. Each section is quantified to illustrate the number of shared and distinct DEGs. (For interpretation of the references to color in this figure legend, the reader is referred to the web version of this article.)

the SSA treatment group, 8 were in the AMB group, and another 8 were in the CTY group. This cluster's phytoplankton densities were significantly higher than the other cluster (ANOVA, $p = 0.0289$). Samples exposed to different concentrations of the same SSA/coast air extract were in one cluster (SSA091, SSA110, SSA134, AMB119), indicating a lack of dose-dependent variation in terms of DEG number was observed. To further elucidate the impact of SSA on mTOR pathway gene expression, samples treated with above-mentioned extracts were compared with NEG group. The resultant upregulation and downregulation of mTOR genes are depicted in a KEGG pathway plot (Fig. 2b), based on log2 fold changes. Our findings reveal that both complexes within the mTOR pathway are modulated following SSA exposure.

2.3. Seasonal variations of SSA composition and exposure effects

As shown in Fig. 1a & SI.11, there are distinct compositional differences between samples collected in colder (Cluster 3 in SI.11) and warmer months (Cluster 2 in SI.11), as indicated by blue and red color bands representing air temperatures within the orange rectangle of SI.11. This variation correlates with the seasonal trends in phytoplankton abundance (see SI.4) and air temperature. We can make a reasonable deduction, higher phytoplankton biomass during warmer periods led to increased concentrations of bioactive chemicals in SSA, and therefore had different expressions compared to the SSA samples collected in colder periods. To further elucidate the impact of seasonal variations on SSA exposure effects, DEGs were calculated again grouping by the SSA sampling date. The number of DEGs varied significantly, with differences up to four magnitudes between samples taken on different dates (Fig. 3a). Notably, there is a strong correlation between the number of DEGs and the phytoplankton density at the time of SSA collection (Fig. 3b). This relationship is particularly pronounced in transcriptome genes, where phytoplankton density accounts for approximately 69 % of the variance in DEG numbers across all samples ($p < 0.01$). Nevertheless, this warrants further investigation to determine effective causality between phytoplankton biogenics in SSA and

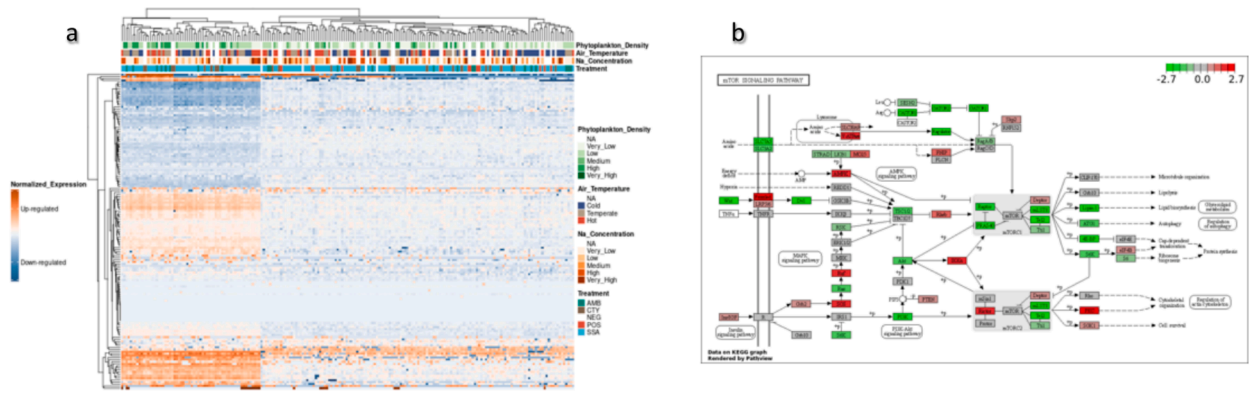

Fig. 2. mTOR pathway response to SSA exposure and environmental conditions. **(a)** Heatmap illustrating gene expression levels across samples, categorized by phytoplankton density, air temperature, sodium concentration, and treatment type. The clustering of gene expression was performed using mTOR-related gene expression profiles and employed the complete linkage method. Metadata annotations below the heatmap were grouped using k-means clustering for binning of sodium concentration (5 clusters), air temperature (3 clusters), and phytoplankton density (4 clusters). Color gradients represent expression levels (blue: down-regulated, red: upregulated). **(b)** KEGG pathway plot indicating specific mTOR pathway genes modulated by SSA exposure, showing both complexes affected, with changes annotated by log2 fold expression differences from controls. (For interpretation of the references to color in this figure legend, the reader is referred to the web version of this article.)

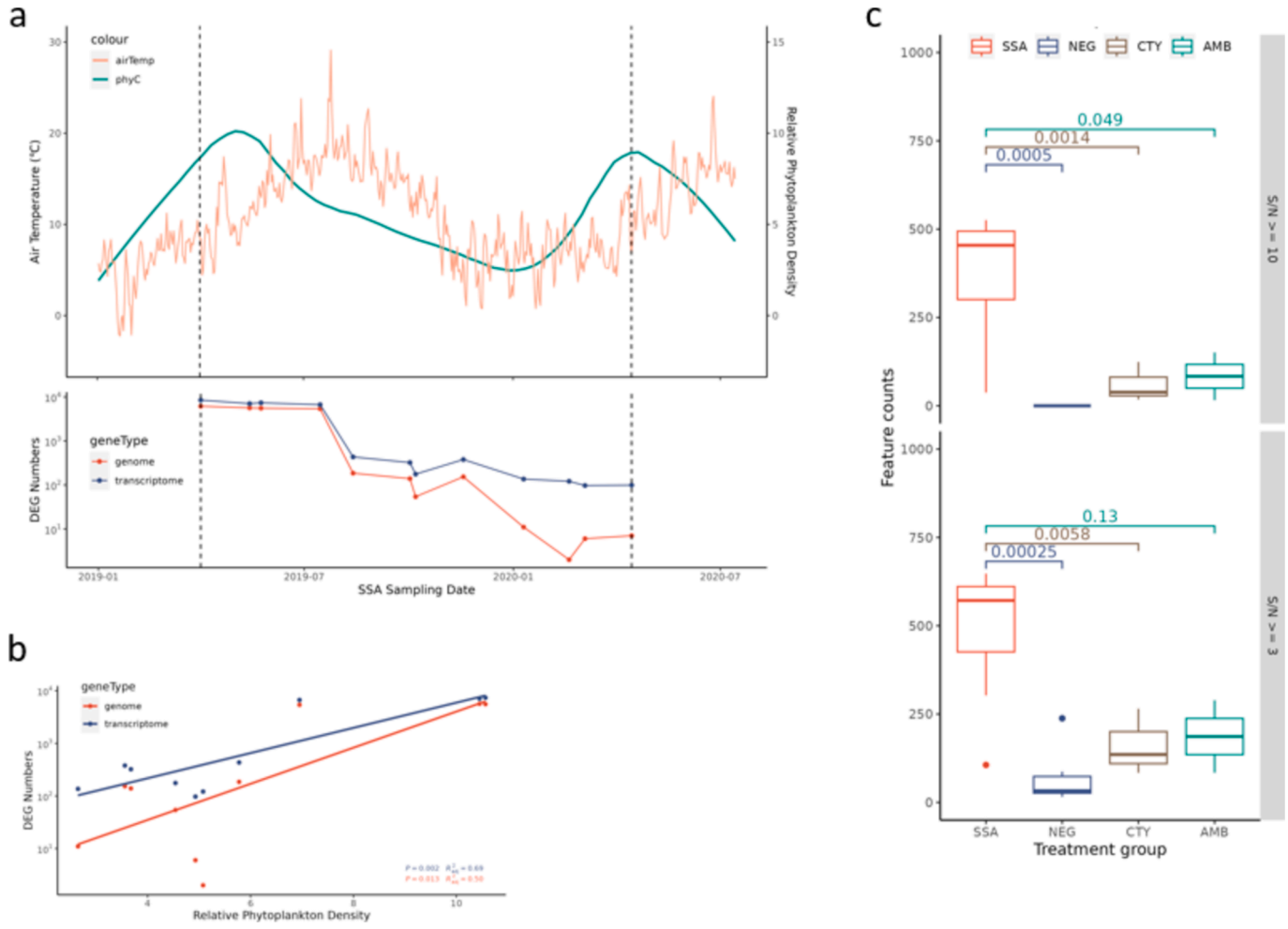

Fig. 3. Seasonal variations of SSA composition and exposure effects. **(a)** Temporal changes in differential gene expression (DEG) numbers over SSA sampling dates, showing distinct shifts along with relative phytoplankton density (PhyC) and air temperature (airTemp) between April 2019 and April 2020. **(b)** Relationship between DEG numbers and relative phytoplankton density, indicating a strong correlation with both genomic and transcriptomic responses. **(c)** Feature counts (the number of distinct signals detected by the mass spectrometer that exceed specified signal-to-noise (S/N) thresholds) across treatment groups, with SSA showing significantly higher diversity in chemical composition than negative control (NEG), ambient air (AMB), and city air (CTY)groups.

potential human health impact.

The chemical diversity within aerosol samples was quantified and analyzed to understand the variation in SSA exposure effects. Using ANOVA and post-hoc comparisons, we found that the SSA group samples exhibited significantly higher feature counts, indicating greater chemical diversity, compared to control groups (Fig. 3c; ANOVA, $p < 0.01$; Tukey HSD results in SI.6). Further, linear regression analysis supports this observation, with a t-value of 2.571 and a p-value of 0.0213, highlighting the distinctive chemical composition of SSA group.

3. Discussions

3.1. Bioactive chemicals in SSA may be released by phytoplankton

Strong correlations between DEG numbers and the phytoplankton densities of the sampling area were observed in our results (Fig. 3b), suggesting the bioactive components in SSA which caused gene differential expressions might originate from the phytoplankton. It is noteworthy that the phytoplankton densities in April of 2019 and 2020 showed differences in terms of trend and values, likely due to annual environmental variations in the sampling area that affect biological diversity, as demonstrated in Fig. 3a. The DEG number trends seem to follow the phytoplankton density trends but with a lag phase around 4 days (SI.7 & SI.8, lag = 4 days, decrease of phytoplankton aligned to DEG number change). A similar pattern is reported in a one-year study (Van Acker et al., 2021a) on SSA chemical composition, it observed a 6-day lag phase between phospholipid (DPPC) concentration in SSA and the decreasing of phytoplankton abundance. This may be explained by the phytoplankton cell lysis a few days after the death, and it takes another few days to be enriched and transported to the coast air. If this holds true, the concentrations of bioactive chemicals in SSA may not be directly linked to the abundance of phytoplankton, but rather to the quantity of deceased phytoplankton from a few days prior. However, since the sampling dates of SSA are approximately one month apart rather than one week, we are not able to use modeling to confirm this hypothesis.

According to several systematic reviews on algal-derived anti-inflammatory or anti-cancer compounds, the bioactive chemical(s) responsible for the exposure effects may belong to the groups of phytosterols, polysaccharides, and polyphenols (Alves et al., 2018; Esposito et al., 2022; Tan et al., 2021). These groups provide us with directions for future exploration of beneficial bioactive substances in SSA, potentially leading to the discovery of substances or drugs that contribute to the improved health of individuals living in the “blue spaces”. The chemical diversity of SSA samples significantly decreased in May and June 2019 (see SI.9), coinciding with the spring blooming of 2019. We hypothesize that the decreased species evenness during the bloom led to a reduction in chemical diversity of the released bioactive chemicals, despite the (delayed) overall rise in the concentration of bioactive chemical(s) in both the water column and SSAs due to the increased biomass.

Although existing studies (May et al., 2018b; Pierce et al., 2003; Zhang and Du, 2017) have demonstrated that higher concentrations of toxins are present in SSA when HABs occur, and DEG numbers after SSA exposure are correlated with the abundances of phytoplankton in seawater in this study, it is currently insufficiently demonstrated that the bioactive substances responsible for DEG number variations originate from phytoplankton. Studies (Santander et al., 2022; Sloth Nielsen et al., 2018) have indicated that air temperature and sea surface temperature are important factors influencing the enrichment factors of hydrophobic components in SSML or SSA. Therefore, the observed interannual variations of DE may also be attributed to the temperature-induced changes in the enrichment factor of bioactive substances in SSA (Fig. 3a & Fig. 3b). Moreover, other marine organisms like bacteria and zooplankton, exhibiting similar temperature-correlated trends, cannot be discounted as alternative bioactive substance sources. Because they all track the same interannual variation trend, it is not possible to verify through the collection of natural samples and exposure experiments conducted in this study. Consequently, controlled Marine Aerosol Reference Tank (MART) experiments, varying marine organisms, are necessary to pinpoint the specific sources of these bioactive substances.

3.2. Implications of SSA exposure on key biological pathways

Our findings from the spring 2019 SSA exposure (April to July) revealed distinct molecular responses compared to control groups (Fig. 2a & Fig. 3a). Notably, there was a significant inhibition of the mTOR pathway (as shown in Fig. 2b), PI3K, Akt, and NF-kB (detailed in the SI.5), alongside a marked activation of the AMPK signaling pathway (SI.5). These molecular changes mirror aspects of bioactive substances produced by algae, which have been reported to either inhibit PI3k/Akt/mTOR/NF-kB (Kim et al., 2015; Walter et al., 2022; Zhao et al., 2020) or activate AMPK (Eo et al., 2015). These five signaling pathways are often associated with cancer, diabetes, and obesity (Moore, 2015), and there are currently many inhibitors targeting these specifics signaling pathways available as drugs or still in clinical trials (Peng et al., 2022). The mTOR, PI3K, and Akt pathways are heavily implicated in cancer development and progression, and their inhibition is often associated with reduced cell proliferation and increased apoptosis (Esposito et al., 2022; Peng et al., 2022). NF-kB is a key regulator of inflammation, and its downregulation suggests that SSA exposure may have anti-inflammatory properties (Kim et al., 2015). AMPK is a central regulator of energy homeostasis that modulates numerous metabolic pathways. Activation of AMPK can enhance insulin sensitivity and is a target for diabetes and obesity treatments (Crunkhorn, 2021; Eo et al., 2015; Esposito et al., 2022; Liu et al., 2021; Peng et al., 2022). In summary, the gene-level responses to the SSA exposure demonstrated potential positive effects on cancer prevention, anti-inflammatory, and metabolic benefits.

3.3. Limitations

We observed effects between AMB group and NEG control, which share the same trend as SSA group, i.e. the presence of wind or not during sampling period does not affect the effects of exposure, this result is not what we expected but can be explained. The smaller SSA particles (majorly developed from film drops) contain a much higher proportion of organic carbon, which contains the bioactive parts of SSA, while the bigger ones mainly contain sea salts (Bertram et al., 2018). Smaller SSA particles also have lower settling velocities, making them more prone to suspension in the air. Literature reports indicate that they sampled SSA particles generated more than 72 h earlier at a distance of 700 km from the nearest seawater source (May et al., 2018a). Analysis of backward trajectories (see SI.10) shows that, except for one SSA sampling date (2019–04-01), all sampling dates involved air masses passing over seawater regions. These trajectory results support the hypothesis that AMB samples may also contain the bioactive components of SSA. This suggests that even in windless conditions, we might collect film drops produced a day or even earlier before sampling. Therefore, the consistent results between the AMB and SSA group in our study are plausible. In future research, it is necessary to incorporate trajectory tracking of the sampling period and location into the model for comprehensive consideration, rather than relying solely on the in-situ wind speed or the content of Na^+ to determine the aerosol sampling concentration.

While our study found a significant correlation between the number of differentially expressed genes (DEGs) and phytoplankton densities in the sampling area, we acknowledge that this correlation alone does not provide strong enough evidence to conclusively support the impact of bioactive chemicals in sea spray aerosols (SSA) released by phytoplankton. The chemical composition of SSA is complex and not fully characterized in our study, making it a “black box” that limits our ability to pinpoint specific bioactive compounds responsible for the observed

biological effects. Additionally, other environmental factors not accounted for could contribute to DEG variability. Without direct chemical analyses linking specific phytoplankton-derived compounds in SSA to gene expression changes, the evidence remains correlational rather than causal. Future studies should focus on isolating and identifying the bioactive components within SSA and assessing their direct effects on gene expression to strengthen the understanding of how phytoplankton activity may influence human health through aerosol exposure.

We are aware that methanol can influence cellular metabolism, and solvent extraction may impact results by enhancing or diminishing the bioactivity of chemical substances (Erukainure et al., 2016). Although our blank control group underwent the same extraction method on unsampled QMA filters, comparing the RNA expression levels between the treatment groups and the blank control group allows us to remove the effects caused by methanol itself. However, the blank control group cannot eliminate the interactive effects between methanol and other bioactive components, as well as the extraction bias caused by the polarity of the solvent. Since we don't know which bioactive chemical(s) substance is responsible for the observed effects, further research is required for clarification. In our research, we focused only on methanol extracted compounds because they are most likely to be enriched during the formation of SSA (Cravigan et al., 2020; Van Acker et al., 2021b) and are more likely to be captured by human respiratory system (Van Acker et al., 2021a).

While our results provide insights into the molecular mechanisms underlying the exposure effects of SSA, it is also important to note that the effects on gene level do not necessarily translate to effects on cell level or above. The transition from in-vitro to in-vivo is a complex process that requires additional studies to determine whether the observed gene-level responses translate into meaningful physiological effects.

Cell viability assays were not conducted at the end of the treatment because the primary focus was the transcriptional profiling of SSA rather than assessing cytotoxicity or cell health per se. While cell viability can be a valuable parameter in certain experimental contexts, RNA integrity was prioritized here as a more direct and relevant measure of experimental validity. All RNA samples exhibited high-quality RIN scores with no degradation, indicating that the cells were in a suitable state for transcriptomic analysis. The experimental design incorporated appropriate controls and biological replicates to address potential variability. Additionally, previous studies on individual compounds present in SSA included comprehensive analyses of cell viability for each compound. Pervious study (van Acker et al., 2020) reported effect concentrations (EC_{10}) ranging from approximately 1 μg/L up to 100 μg/L or even more than 1000 μg/L, depending on the compound. Furthermore, prior exposure data for some of these compounds showed their concentrations in the range of picograms per cubic meter of air (Van Acker et al., 2021b), which are much lower than any reported effect data. Taken together, these findings suggest that limited effects on cell viability were expected. RNA integrity was used as a measure to ensure high-quality extractions with minimal impact on cell viability. Nevertheless, potential mixture effects affecting cell viability cannot be entirely excluded. Therefore, no conclusions regarding the potential impact on cell viability are made, as this was not tested.

Another limit of our study is the time interval for our SSA sample collection, which is approximately one month in between each sampling date. This is insufficient to track the rapid changes in planktonic communities, especially during spring and summer algal blooming. If future studies can collect samples on a weekly basis during the spring algal bloom period and a few (e.g. four) days after, they may draw more compelling conclusions.

4. Conclusions

The research presented in this article is, to the best of our knowledge, the first study to expose human lung epithelial (BEAS-2B) cells to natural SSAs at environmentally relevant concentrations and investigate their molecular-level health effects. In this research we have the following findings: 1. Under normal environmental conditions, exposure to natural SSA can influence the RNA expression of BEAS-2B cells, including the inhibition of the PI3k/Akt/mTOR/NF-kB signaling pathway and the activation of the AMPK signaling pathway. 2. The bioactive components of SSA responsible for the effects may be influenced by algal activity, with the most pronounced effects observed during spring algal blooms. 3. Air samples collected during no wind conditions may also contain these bioactive components, potentially originating from previously generated SSA or from distant sources.

5. Methods

5.1. Aerosol sampling and chemical extractions

The sea spray aerosol sampling campaign was conducted from 1st April 2019 until 14th April 2020 on the beach of Ostend, Belgium (51.239°N, 2.931°E). The aerosol sampling method followed Van Acker et al. (2021a) except the collected air volume of each aerosol sample was fixed to approximately 2000 L instead of collecting for a fixed period. Briefly, for each aerosol sample, an acid-washed (1 % HNO_3) QM-A quartz microfiber filter (Whatman, Ø 47 mm, air retention 99.95 % for 0.3 μm particle) was placed in a cleaned stainless-steel in-line filter holder (Pall Corporation) and connected to a constant airflow sample pump (Leland Legacy, SKC Inc.). During the sampling, the filter holders were placed on a tripod within 15 m of the waterline and the tripod was moved frequently to maintain the same distance to waterline. (following the tide). The height of filter holders was around 1.6 m and the front openings of the filter holders were facing the direction from which the wind was blowing. The pumps were set at an airflow rate of 10 ~ 12 L min^{-1} until 2000 L of air containing SSA was sampled on the filters. In-situ average and gust wind speeds were measured using a wind meter before and after the sampling. The sampling days were chosen based on the weather conditions. We only took SSA samples when there was no precipitation and the wind was blowing from the sea. According to literature, SSA production occurs at speeds above 4 m/s (Gantt et al., 2011; Lewis and Schwartz, 2004; O'Dowd and De Leeuw, 2007). In this campaign, 12 SSA samples were collected, three of them were collected at wind speeds lower than 3 m/s when the wind was blowing form inland. These samples were considered as ambient coastal aerosol samples (AMB). For each sampling day, an extra filter was taken through the exact same procedure as the aerosol sample filters except it was not connected to the pump and was used as a blank control. In addition to the SSA and AMB aerosol samples, three city aerosol samples (CTY) were taken with the same sampling system in Ghent University Campus Coupure, Ghent Belgium (51.053°N, 3.707°E) on the roof of a 12 m heigh building. This city's location is around 40 km away from the coastline. The detailed time and environmental information are listed in the SI.1.

The filter samples were first cut into two pieces with scissors rinsed with 1 % HNO_3: 1/4 and 3/4 separately. (I) The 1/4 parts were used for Inductively Coupled Plasma – Optical Emission Spectroscopy (ICP-OES, Thermo Scientific iCAP 7000 series) analysis to measure the concentrations of Na^+ and Mg^+ in the SSA samples and Na^+ was used as a proxy quantifier of the SSA content in a sample (Lewis and Schwartz, 2004) and Na^+/Mg^+ ratio was used to confirm the source of SSA. The filter parts were placed in falcon tubes with 5 mL 1 % HNO_3, vortexed, and sonicated to elute Na^+ and Mg^+ from the filter. The elution step was repeated three times, resulting in a 15 ml extract solution for each sample. Extracts were then filtered over 0.45 μm (Supor filter, Cytiva) to remove filter debris generated during elution and stored at 4 °C until analysis. (II) The 3/4 parts were extracted for the exposure experiment: The extraction method used was based on the dedicated extraction protocols of Ullah et al. (2015) and optimized by Van Acker et al.

(2021b). Methanol was used as eluent, and the elution step was repeated twice (10 mL and 3 mL), resulting in a 13 mL extract for each sample. Afterward, extracts were filtered by 0.2 μm polytetrafluoroethylene (PTFE) syringe filters (Phenex) and dried under a gentle N_2 stream at 40 °C until around 1 mL extracts were obtained and reconstituted in 1.628 mL methanol. The filter extracts were subsequently stored at −20 °C until they were used as treatments in the vitro experiment.

5.2. Cell culture and exposure experiment

In the in vitro experiment, a human bronchial epithelial cell line (BEAS-2B) obtained from the Laboratory of Experimental Cancer Research at Ghent University was utilized. The use of this cell line was conducted in compliance with ethical standards, having received approval from the ethical commission under the reference number EC/2019/1856. Additionally, the cell line is registered with the Federal Agency for Medicines and Health Products of Belgium (FAGG) biobank with the identification number BB200014. Cells were cultured in Dulbecco's modified eagle medium (DMEM), supplemented with 10 % fetal bovine serum (FBS), 100 units mL^{-1} penicillin, and 100 μg mL^{-1} streptomycin. Cell cultures were grown in a humidified incubator at 37 °C, 5 % CO2, and > 95 % relative humidity. Confluent cultures were sub-cultured, using 0.5 % Trypsin–EDTA, and split two times per week in a 1:6 ratio. Passage numbers of the cell culture were limited to less than 50. Confluent cell cultures were trypsinized and seeded in six-well plates at a density of 320,000 cells $well^{-1}$ with 3 mL fresh DMEM, followed by 10 h incubation at the same conditions as mentioned above.

The cells were exposed to one of the treatments listed in Table 1. and then incubated for another 48 h prior to RNA extraction, the time length of exposure was the maximum duration without splitting the cells. To simulate environmentally relevant exposure conditions in our in vitro experiments, we calculated the doses of aerosol treatments by proportionally scaling the concentration of aerosol extracts based on the ratio of the total human alveolar surface area to the alveolar surface area exposed in our cell culture model under different environmental exposure conditions including inhalation volume and increased aerosolization. This method was also used by Asselman et al. (2019). The doses of exposure treatments were calculated based on the human Alveolar surface as Formula (1) using the principle in toxicology of geometric progression with a constant factor of 2.

Table 1
Summary of treatment groups and sample information.

Exposure type	Concentration levels	Num. of aerosol samples/ chemicals	Num. of treatments	Num. of cellline samples
Sea spray aerosol (SSA)	x10 x20 x40 x80	9	36	144
Ambient coast aerosol (AMB)	x10 x80	3	6	24
City aerosol (CTY)	x10 x80	3	6	24
Negative control (NEG)	x1	1	1	4
Positive control (POS)	x1	1	1	12
Total		17	50	208

Note: Concentration levels refer to the calculated exposure doses, expressed as multiplicative factors (M = 10, 20, 40, or 80), which simulate environmentally relevant exposure conditions in vitro. These factors were derived by proportionally scaling aerosol extract concentrations based on the ratio of total human alveolar surface area to the alveolar surface area exposed in the cell culture model. The dose calculation is detailed in the methods section under "Formula (1)". For the positive control (POS), the concentration represents the use of 0.1 μM mTOR kinase inhibitor PP242. All treatments were performed in four replicates unless specified otherwise.

$$M = \frac{(T_s \times DF)/A_e}{T_{e/A_h}} \quad (1)$$

Calculation of dilution factors used for aerosol extracts.

***M**: the multiplicative factor by which the environmental condition is multiplied to achieve the desired exposure dose, in this research we have M = 10, 20, 40, or 80. **T_e**: the total duration for which the cells were exposed to the aerosol extracts. **T_s**: the duration for which the aerosol sample was collected. **A_e**: the calculated alveolar surface area exposed, in this research $A_e = 9.6\ cm^2$. **A_h**: the total human alveolar surface area which is $4 \times 10^5\ cm^2$. **DF**: the dilution factor, in this research we used 289, 145, 72, or 36 for different M.*

A known mTOR kinase inhibitor Torkinib or PP242 (MedChemExpress) was used as the positive control (POS) at concentration of 0.1 μM. The negative control (NEG) also contained 2 % methanol to exclude a solvent effect as all other treatments were extracted, diluted, or dissolved in methanol.

In the in vitro experiment, we exposed BEAS-2B cells to (1) SSA samples (SSA) (2) ambient coast aerosol samples (AMB, where there was no wind during the sampling), (3) city aerosol samples (CTY), (4) positive controls (POS), and (5) negative controls (NEG). For each aerosol/control sample, several different concentrations were used for exposure, resulting in 50 treatments (aerosol sample − concentration combination) with 17 different aerosol samples or chemicals. Every treatment consists of four replicas (with two exceptions noted in the remarks). The number of cell line samples in this research is 208. A summary of treatment groups and sample information is listed in Table 1. A detailed cell line sample list is attached in the SI.2.

5.3. RNA extraction and sequencing

RNA was extracted using the Qiagen RNEasy kit following the manufacturer's instructions including DNAse digestion. Quality and concentration of the input total RNA was checked with 'Quant-it ribogreen RNA assay' (Life Technologies, Grand Island, NY, USA) and the RNA 6000 nano chip (Agilent Technologies, Santa Clara, CA, USA), respectively. The RIN values were 9.01 ± 0.85 (average ± standard deviation). Subsequently, 48 ng of RNA was used to perform an Illumina sequencing library preparation using the QuantSeq 3′ mRNA-Seq Library Prep FWD Kit (Lexogen, Vienna, Austria) including Unique Molecular Identifiers (UMI) according to the manufacturer's protocol using 14 enrichment PCR cycles. Libraries were quantified by qPCR, according to Illumina's protocol 'Sequencing Library qPCR Quantification protocol guide'. A High sensitivity DNA chip (Agilent Technologies, Santa Clara, CA, US) was used to control the library's size distribution and quality. Based on Illumine sequencing guidelines, the libraries are first normalized to the same concentration, then equal volumes are pooled to yield a pool of the same concentration of each of the original normalized libraries. Libraries were then sequenced on an Illumina Hiseq sequencer together with 2 % PhiX Sequencing Control library, generating 50 bp single-end reads.

5.4. Laser-assisted ambient ionization mass spectrometry (LA-REIMS) analyses

LA-REIMS was used for the chemical analysis of our aerosol samples. This untargeted approach was chosen given the undefined nature of potential compounds of interest, providing a comprehensive fingerprinting of the samples, which may be useful in future studies. Initial analyses were performed by ProDigest BV (Belgium) using established methodology (Van Meulebroek et al., 2020). The LA-REIMS platform utilized a MID infrared laser system (OpoletteTM HE2940, OPOTEK, LLC, USA) that consisted of a Q-switched Nd:YAG laser pumping an Optical Parametric Oscillator (OPO). The transmission of the laser energy into the sample was achieved through free space optics, which

included a series of metallic-coated mirrors and a Plano-convex lens. The process of laser ablation, performed for 3 s per sample, is initiated based on the laser-emitted infrared wavelength regime that excites the most intense vibrational band of the water molecules contained by the sample. This leads to matrix-assisted desorption and ionization of intact biomolecules. The produced aerosol is then transferred to the REIMS platform. Mass analysis was conducted using a Xevo G2-XS Quadrupole Time-of-Flight (QToF) mass spectrometer, operated in negative ionization mode with an m/z scan range of 50–1200 Da, obtaining relative intensities for each sample. An external standard (leucine-enkephalin, 0.25 ng/μL) was used for lock mass correction and signal intensity drift correction. For the purpose of distinguishing true signals from noise, a noise value was established using the mean relative intensities of blank samples augmented by 0.001. Features were then distinguished based on signal-to-noise (S/N) ratios, employing thresholds of both 3 and 10, thereby representing the chemical diversity of each sample.

5.5. Data analyses

Poly-A and Illumina Truseq RNA adapters are trimmed according to the manufacturer (Lexogen, QuantSeq 3'mRNA-Seq Data Analysis) using bbduck.sh in BBMap package version 35.85 (Bushnell et al., 2017). We used STAR version 2.7.9a (Dobin et al., 2013) to align the sequences, using the human Genome Reference Consortium build 38 (GRCh38) (Cunningham et al., 2015) as alignment reference genome. We used the same parameters as the manufacturer suggested, except we did not specify the SAM attributes (outSAMattributes), so the output BAM files have the default attributes (NH HI AS nM). We used StringTie version 2.1.6 (Pertea et al., 2015) for the assembly of the aligned read sequences. In this process, we supplied only the reference genome, specifically the gene annotation file (Homo_sapiens.GRCh38.89.gtf) obtained from Ensembl (Martin et al., 2023), along with the designated file paths for input and output. All other parameters were left at their default settings. RPKM counts are extracted using the getFPKM.py provided by StringTie.

We use R version 4.1.2 (R Core Team, 2014) as the general software platform for statistical analyses and visualizations. The ggplot2 version 3.3.5 (Wickham, 2009) was used as the main tool for generating figures. Differential gene expression analysis between treatment groups (SSA, AMB, CTY, POS) and negative control (NEG) was performed using DESeq function in package DESeq2 version 1.32.0 (Love et al., 2014) with build-in batch effect calibration and default parameters. Normalized counts were generated using counts function in package DESeq2, median absolute deviation (MAD) was then used to rank normalized counts, ensuring robust statistical comparison. The False Discovery Rate (FDR) and Log2 Fold Change (Log2FC) were used to screen for DEGs, thresholds were determined according to the applications and were mentioned in related figures. Filters for protein-coding genes were generated based on the same reference genome GRCh38 as for alignments. The Euclidean distances between each sample's gene expression were calculated and subsequently clustered using the centroid algorithm for unsupervised hierarchical clustering. We used the Kyoto Encyclopedia of Genes and Genomes (KEGG) (Ogata et al., 1999) database for annotating the gene functions and signaling pathways. Enrichment analyses were performed by clusterProfiler version 4.0.5 (Yu et al., 2012) with P-value cutoff at 0.01. The data for plotting the dendrogram was computed with hierarchical cluster analysis using R's built-in *hclust* function with centroid algorithm. Analysis of variance (ANOVA) was conducted on phytoplankton densities and chemical diversity with the *aov* function. Homogeneity of variance was checked with the *vif* function from the *car* package (version 3.1–2) and normality was assessed with Shapiro-Wilk tests using *shapiro.test* function. For chemical diversity, post-hoc comparisons between different treatments were made using the *TukeyHSD* function. A generalized linear model was fitted using *glm* function to determine the sources of variation in the number of DEGs. Aerosol backward trajectories were calculated using the SplitR package in R with the HYSPLIT split model to identify potential sources of aerosol particles impacting the sampling site.

6. Disclaimer

The authors would like to clarify that this manuscript utilized the assistance of ChatGPT, an AI language model developed by OpenAI, for the sole purpose of spelling and grammar checks. No content, analytical insights, or scientific conclusions were derived from or influenced by this AI tool. All substantive research, findings, and conclusions presented in this paper are the original work of the authors.

Data availability statement

The RNA sequencing raw data supporting the findings of this study will be uploaded to the National Center for Biotechnology Information (NCBI) Sequence Read Archive (SRA) and can be accessed using the designated accession number PRJNA1070847. The raw data from the Laser-Assisted Rapid Evaporative Ionisation Mass Spectrometry (LA-REIMS) analyses are available from the corresponding author upon reasonable request. All other relevant data are within the paper and its Supporting Information files.

CRediT authorship contribution statement

Zixia Liu: Writing – review & editing, Writing – original draft, Software, Methodology, Data curation. **Emmanuel Van Acker:** Writing – review & editing, Methodology, Data curation, Conceptualization. **Maarten De Rijcke:** Writing – review & editing, Methodology, Conceptualization. **Filip Van Nieuwerburgh:** Writing – review & editing, Methodology. **Colin Janssen:** Writing – review & editing, Supervision, Conceptualization. **Jana Asselman:** Writing – review & editing, Supervision, Methodology, Conceptualization.

Declaration of competing interest

The authors declare that they have no known competing financial interests or personal relationships that could have appeared to influence the work reported in this paper.

Acknowledgements

The authors acknowledge Jolien Depecker, Emmy Pequeur, Illias Semmouri for their assistance during the experiment, Nancy De Saeyer, and the staff of nxtgnt for their technical assistance. The cell lines have been originally set up in collaboration with Ilse Beck, Karlien Van Wesemael, and Marc Bracke from the Laboratory of Experimental Cancer Research (UGent). Zixia Liu has been awarded a CSC scholarship (CSC No.201906100034). Jana Asselman was awarded a Research Grant of the Ghent University Research Fund BOFSTG2020001201.

Appendix A. Supplementary data

Supplementary data to this article can be found online at https://doi.org/10.1016/j.envint.2025.109255.

Data availability

Data will be made available on request.

References

Aller, J.Y., Kuznetsova, M.R., Jahns, C.J., Kemp, P.F., 2005. The sea surface microlayer as a source of viral and bacterial enrichment in marine aerosols. J. Aerosol Sci 36, 801–812. https://doi.org/10.1016/j.jaerosci.2004.10.012.

Alves, C., Silva, J., Pinteus, S., Gaspar, H., Alpoim, M.C., Botana, L.M., Pedrosa, R., 2018. From marine origin to therapeutics: The antitumor potential of marine algae-derived

compounds. Front. Pharmacol. 9, 353805. https://doi.org/10.3389/FPHAR.2018.00777/BIBTEX.
Asselman, J., Van Acker, E., De Rijcke, M., Tilleman, L., Van Nieuwerburgh, F., Mees, J., De Schamphelaere, K.A.C., Janssen, C.R., 2019. Marine biogenics in sea spray aerosols interact with the mTOR signaling pathway. Sci. Rep. 9, 675. https://doi.org/10.1038/s41598-018-36866-3.
Ault, A.P., Moffet, R.C., Baltrusaitis, J., Collins, D.B., Ruppel, M.J., Cuadra-Rodriguez, L. A., Zhao, D., Guasco, T.L., Ebben, C.J., Geiger, F.M., Bertram, T.H., Prather, K.A., Grassian, V.H., 2013. Size-dependent changes in sea spray aerosol composition and properties with different seawater conditions. Environ. Sci. Tech. 47, 5603–5612. https://doi.org/10.1021/ES400416G/SUPPL_FILE/ES400416G_SI_001.PDF.
Backer, L.C., Kirkpatrick, B., Fleming, L.E., Cheng, Y.S., Pierce, R., Bean, J.A., Clark, R., Johnson, D., Wanner, A., Tamer, R., Zhou, Y., Baden, D.G., 2005. Occupational exposure to aerosolized brevetoxins during Florida red tide events: Effects on a healthy worker population. Environ. Health Perspect. 113, 644–649. https://doi.org/10.1289/ehp.7502.
Bar-On, Y.M., Milo, R., 2019. The Biomass Composition of the Oceans: A Blueprint of Our Blue Planet. Cell 179, 1451–1454. https://doi.org/10.1016/j.cell.2019.11.018.
Bell, S.L., Phoenix, C., Lovell, R., Wheeler, B.W., 2015. Seeking everyday wellbeing: The coast as a therapeutic landscape. Soc Sci Med 142, 56–67. https://doi.org/10.1016/J.SOCSCIMED.2015.08.011.
Bertram, T.H., Cochran, R.E., Grassian, V.H., Stone, E.A., 2018. Sea spray aerosol chemical composition: elemental and molecular mimics for laboratory studies of heterogeneous and multiphase reactions. Chem. Soc. Rev. 47, 2374–2400. https://doi.org/10.1039/C7CS00008A.
Bushnell, B., Rood, J., Singer, E., 2017. BBMerge – Accurate paired shotgun read merging via overlap. PLoS One 12, e0185056. https://doi.org/10.1371/JOURNAL.PONE.0185056.
Cheng, Y.S., Zhou, Y., Naar, J., Irvin, C.M., Su, W.C., Fleming, L.E., Kirkpatrick, B., Pierce, R.H., Backer, L.C., Baden, D.G., 2010. Personal exposure to aerosolized red tide toxins (brevetoxins). J. Occup. Environ. Hyg. 7, 326–331. https://doi.org/10.1080/15459621003724041.
Cochran, R.E., Laskina, O., Trueblood, J.V., Estillore, A.D., Morris, H.S., Jayarathne, T., Sultana, C.M., Lee, C., Lin, P., Laskin, J., Laskin, A., Dowling, J.A., Qin, Z., Cappa, C. D., Bertram, T.H., Tivanski, A.V., Stone, E.A., Prather, K.A., Grassian, V.H., 2017. Molecular Diversity of Sea Spray Aerosol Particles: Impact of Ocean Biology on Particle Composition and Hygroscopicity. Chem 2, 655–667. https://doi.org/10.1016/J.CHEMPR.2017.03.007.
Cravigan, L.T., Mallet, M.D., Vaattovaara, P., Harvey, M.J., Law, C.S., Modini, R.L., Russell, L.M., Stelcer, E., Cohen, D.D., Olsen, G., Safi, K., Burrell, T.J., Ristovski, Z., 2020. Sea spray aerosol organic enrichment, water uptake and surface tension effects. Atmos. Chem. Phys. 20, 7955–7977. https://doi.org/10.5194/acp-20-7955-2020.
Crunkhorn, S., 2021. A new route to regulating AMPK activity. Nat. Rev. Drug Discov. 20, 175. https://doi.org/10.1038/D41573-021-00021-X.
Cunningham, F., Amode, M.R., Barrell, D., Beal, K., Billis, K., Brent, S., Carvalho-Silva, D., Clapham, P., Coates, G., Fitzgerald, S., Gil, L., Girón, C.G., Gordon, L., Hourlier, T., Hunt, S.E., Janacek, S.H., Johnson, N., Juettemann, T., Kähäri, A.K., Keenan, S., Martin, F.J., Maurel, T., McLaren, W., Murphy, D.N., Nag, R., Overduin, B., Parker, A., Patricio, M., Perry, E., Pignatelli, M., Riat, H.S., Sheppard, D., Taylor, K., Thormann, A., Vullo, A., Wilder, S.P., Zadissa, A., Aken, B. L., Birney, E., Harrow, J., Kinsella, R., Muffato, M., Ruffier, M., Searle, S.M.J., Spudich, G., Trevanion, S.J., Yates, A., Zerbino, D.R., Flicek, P., 2015. Ensembl 2015. Nucleic Acids Res. 43, D662–D669. https://doi.org/10.1093/nar/gku1010.
DeMott, P.J., Hill, T.C.J., McCluskey, C.S., Prather, K.A., Collins, D.B., Sullivan, R.C., Ruppel, M.J., Mason, R.H., Irish, V.E., Lee, T., Hwang, C.Y., Rhee, T.S., Snider, J.R., McMeeking, G.R., Dhaniyala, S., Lewis, E.R., Wentzell, J.J.B., Abbatt, J., Lee, C., Sultana, C.M., Ault, A.P., Axson, J.L., Martinez, M.D., Venero, I., Santos-Figueroa, G., Stokes, M.D., Deane, G.B., Mayol-Bracero, O.L., Grassian, V.H., Bertram, T.H., Bertram, A.K., Moffett, B.F., Franc, G.D., 2016. Sea spray aerosol as a unique source of ice nucleating particles. PNAS 113, 5797–5803. https://doi.org/10.1073/PNAS.1514034112/SUPPL_FILE/PNAS.1514034112.SD01.PDF.
Dobin, A., Davis, C.A., Schlesinger, F., Drenkow, J., Zaleski, C., Jha, S., Batut, P., Chaisson, M., Gingeras, T.R., 2013. STAR: Ultrafast universal RNA-seq aligner. Bioinformatics 29, 15–21. https://doi.org/10.1093/BIOINFORMATICS/BTS635.
Dong, H., Dong, S., Erik Hansen, P., Stagos, D., Lin, X., Liu, M., 2020. Progress of bromophenols in marine algae from 2011 to 2020: Structure, bioactivities, and applications. Mar. Drugs 18, 411. https://doi.org/10.3390/md18080411.
Eo, H., Jeon, Y.J., Lee, M., Lim, Y., 2015. Brown alga Ecklonia cava polyphenol extract ameliorates hepatic lipogenesis, oxidative stress, and inflammation by activation of AMPK and SIRT1 in high-fat diet-induced obese mice. J. Agric. Food Chem. 63, 349–359. https://doi.org/10.1021/JF502830B/ASSET/IMAGES/LARGE/JF-2014-02830B_0007.JPEG.
Erukainure, O.L., Ebuehi, O.A.T., Iqbal Chaudhary, M., Mesaik, M.A., Shukralla, A., Muhammad, A., Zaruwa, M.Z., Elemo, G.N., 2016. Orange peel extracts: Chemical characterization, antioxidant, antioxidative burst, and phytotoxic activities. J Diet Suppl 13. https://doi.org/10.3109/19390211.2016.1150932.
Esposito, R., Federico, S., Glaviano, F., Somma, E., Zupo, V., Costantini, M., 2022. Bioactive compounds from marine sponges and algae: Effects on cancer cell metabolome and chemical structures. Int. J. Mol. Sci. 23, 10680. https://doi.org/10.3390/IJMS231810680.
Fleming, L.E., Backer, L.C., Baden, D.G., 2005. Overview of aerosolized florida red tide toxins: Exposures and effects. Environ. Health Perspect. 113, 618–620. https://doi.org/10.1289/ehp.7501.
Fleming, L.E., Bean, J.A., Kirkpatrick, B., Cheng, Y.S., Pierce, R., Naar, J., Nierenberg, K., Backer, L.C., Wanner, A., Reich, A., Zhou, Y., Watkins, S., Henry, M., Zaias, J., Abraham, W.M., Benson, J., Cassedy, A., Hollenbeck, J., Kirkpatrick, G., Clake, T., Baden, D.G., 2009. Exposure and effect assessment of aerosolized red tide toxins (Brevetoxins) and asthma. Environ. Health Perspect. 117, 1095–1100. https://doi.org/10.1289/ehp.0900673.
Gantt, B., Meskhidze, N., Facchini, M.C., Rinaldi, M., Ceburnis, D., O'Dowd, C.D., 2011. Wind speed dependent size-resolved parameterization for the organic mass fraction of sea spray aerosol. Atmos. Chem. Phys. 11, 8777–8790. https://doi.org/10.5194/acp-11-8777-2011.
Gascon, M., Mas, M.T., Martínez, D., Dadvand, P., Forns, J., Plasència, A., Nieuwenhuijsen, M.J., 2015. Mental health benefits of long-term exposure to residential green and blue spaces: a systematic review. Int. J. Environ. Res. Public Health 12, 4354–4379. https://doi.org/10.3390/IJERPH120404354.
Gascon, M., Zijlema, W., Vert, C., White, M.P., Nieuwenhuijsen, M.J., 2017. Outdoor blue spaces, human health and well-being: A systematic review of quantitative studies. Int. J. Hyg. Environ. Health 220, 1207–1221. https://doi.org/10.1016/J.IJHEH.2017.08.004.
Hidalgo, A., Cruz, A., Pérez-Gil, J., 2015. Barrier or carrier? Pulmonary surfactant and drug delivery. Eur. J. Pharm. Biopharm. 95, 117–127. https://doi.org/10.1016/J.EJPB.2015.02.014.
Hoagland, P., Jin, D., Polansky, L.Y., Kirkpatrick, B., Kirkpatrick, G., Fleming, L.E., Reich, A., Watkins, S.M., Ullmann, S.G., Backer, L.C., 2009. The costs of respiratory illnesses arising from Florida gulf coast Karenia brevis blooms. Environ. Health Perspect. 117, 1239–1243. https://doi.org/10.1289/EHP.0900645.
Keene, W.C., Maring, H., Maben, J.R., Kieber, D.J., Pszenny, A.A.P., Dahl, E.E., Izaguirre, M.A., Davis, A.J., Long, M.S., Zhou, X., Smoydzin, L., Sander, R., 2007. Chemical and physical characteristics of nascent aerosols produced by bursting bubbles at a model air-sea interface. J. Geophys. Res. Atmos. 112, D21202. https://doi.org/10.1029/2007JD008464.
Kim, M.E., Jung, Y.C., Jung, I., Lee, H.W., Youn, H.Y., Lee, J.S., 2015. Anti-inflammatory Effects of Ethanolic Extract from Sargassum horneri (Turner) C. Agardh on Lipopolysaccharide-Stimulated Macrophage Activation via NF-κB Pathway. Regulation 44, 137–146. https://doi.org/10.3109/08820139.2014.942459.
Lang-Yona, N., Lehahn, Y., Herut, B., Burshtein, N., Rudich, Y., 2014. Marine aerosol as a possible source for endotoxins in coastal areas. Sci. Total Environ. 499, 311–318. https://doi.org/10.1016/j.scitotenv.2014.08.054.
Lewis, E.R., Schwartz, S.E., 2004. In: Sea Salt Aerosol Production: Mechanisms, Methods, Measurements and Models—A Critical Review. Geophysical Monograph Series, Geophysical Monograph Series. American Geophysical Union, Washington, D.C. https://doi.org/10.1029/152GM01.
Liu, Y., Jurczak, M.J., Lear, T.B., Lin, B., Larsen, M.B., Kennerdell, J.R., Chen, Y., Huckestein, B.R., Nguyen, M.K., Tuncer, F., Jiang, Y., Monga, S.P., O'Donnell, C.P., Finkel, T., Chen, B.B., Mallampalli, R.K., 2021. A Fbxo48 inhibitor prevents pAMPKα degradation and ameliorates insulin resistance. Nat. Chem. Biol. 17, 298–306. https://doi.org/10.1038/s41589-020-00723-0.
Love, M.I., Huber, W., Anders, S., 2014. Moderated estimation of fold change and dispersion for RNA-seq data with DESeq2. Genome Biol. 15, 550. https://doi.org/10.1186/s13059-014-0550-8.
Martin, F.J., Amode, M.R., Aneja, A., Austine-Orimoloye, O., Azov, A.G., Barnes, I., Becker, A., Bennett, R., Berry, A., Bhai, J., Bhurji, S.K., Bignell, A., Boddu, S., Branco Lins, P.R., Brooks, L., Ramaraju, S.B., Charkhchi, M., Cockburn, A., Da Rin Fiorretto, L., Davidson, C., Dodiya, K., Donaldson, S., El Houdaigui, B., El Naboulsi, T., Fatima, R., Giron, C.G., Genez, T., Ghattaoraya, G.S., Martinez, J.G., Guijarro, C., Hardy, M., Hollis, Z., Hourlier, T., Hunt, T., Kay, M., Kaykala, V., Le, T., Lemos, D., Marques-Coelho, D., Marugán, J.C., Merino, G.A., Mirabueno, L.P., Mushtaq, A., Hossain, S.N., Ogeh, D.N., Sakthivel, M.P., Parker, A., Perry, M., Piliota, I., Prosovetskaia, I., Perez-Silva, J.G., Salam, A.I.A., Saraiva-Agostinho, N., Schuilenburg, H., Sheppard, D., Sinha, S., Sipos, B., Stark, W., Steed, E., Sukumaran, R., Sumathipala, D., Suner, M.M., Surapaneni, L., Sutinen, K., Szpak, M., Tricomi, F.F., Urbina-Gómez, D., Veidenberg, A., Walsh, T.A., Walts, B., Wass, E., Willhoft, N., Allen, J., Alvarez-Jarreta, J., Chakiachvili, M., Flint, B., Giorgetti, S., Haggerty, L., Ilsley, G.R., Loveland, J.E., Moore, B., Mudge, J.M., Tate, J., Thybert, D., Trevanion, S.J., Winterbottom, A., Frankish, A., Hunt, S.E., Ruffier, M., Cunningham, F., Dyer, S., Finn, R.D., Howe, K.L., Harrison, P.W., Yates, A.D., Flicek, P., 2023. Ensembl 2023. Nucleic Acids Res. 51, D933–D941. https://doi.org/10.1093/NAR/GKAC958.
May, N.W., Gunsch, M.J., Olson, N.E., Bondy, A.L., Kirpes, R.M., Bertman, S.B., China, S., Laskin, A., Hopke, P.K., Ault, A.P., Pratt, K.A., 2018a. Unexpected Contributions of Sea Spray and Lake Spray Aerosol to Inland Particulate Matter. Environ. Sci. Technol. Lett. 5, 405–412. https://doi.org/10.1021/acs.estlett.8b00254.
May, N.W., Olson, N.E., Panas, M., Axson, J.L., Tirella, P.S., Kirpes, R.M., Craig, R.L., Gunsch, M.J., China, S., Laskin, A., Ault, A.P., Pratt, K.A., 2018b. Aerosol Emissions from Great Lakes Harmful Algal Blooms. Environ. Sci. Tech. 52, 397–405. https://doi.org/10.1021/acs.est.7b03609.
Menaa, F., Wijesinghe, U., Thiripuranathar, G., Althobaiti, N.A., Albalawi, A.E., Khan, B. A., Menaa, B., 2021. Marine Algae-Derived Bioactive Compounds: A New Wave of Nanodrugs? Mar. Drugs 19. https://doi.org/10.3390/MD19090484.
Miyazaki, Y., Suzuki, K., Tachibana, E., Yamashita, Y., Müller, A., Kawana, K., Nishioka, J., 2020. New index of organic mass enrichment in sea spray aerosols linked with senescent status in marine phytoplankton. Sci. Rep. 10, 1–9. https://doi.org/10.1038/s41598-020-73718-5.
Moore, M.N., 2015. Do airborne biogenic chemicals interact with the PI3K/Akt/mTOR cell signalling pathway to benefit human health and wellbeing in rural and coastal environments? Environ. Res. 140, 65–75. https://doi.org/10.1016/j.envres.2015.03.015.

O'Dowd, C.D., De Leeuw, G., 2007. Marine aerosol production: A review of the current knowledge. Philos. Trans. R. Soc. A Math. Phys. Eng. Sci. 365, 1753–1774. https://doi.org/10.1098/rsta.2007.2043.

Ogata, H., Goto, S., Sato, K., Fujibuchi, W., Bono, H., Kanehisa, M., 1999. KEGG: Kyoto Encyclopedia of Genes and Genomes. Nucleic. Acids. Res. 27, 29–34. https://doi.org/10.1093/nar/27.1.29.

Peng, Y., Wang, Y., Zhou, C., Mei, W., Zeng, C., 2022. PI3K/Akt/mTOR Pathway and Its Role in Cancer Therapeutics: Are We Making Headway? Front. Oncol. https://doi.org/10.3389/fonc.2022.819128.

Pereira, L., 2018. Seaweeds as Source of Bioactive Substances and Skin Care Therapy—Cosmeceuticals, Algotheraphy, and Thalassotherapy. Cosmetics 5, 68. https://doi.org/10.3390/cosmetics5040068.

Pertea, M., Pertea, G.M., Antonescu, C.M., Chang, T.C., Mendell, J.T., Salzberg, S.L., 2015. StringTie enables improved reconstruction of a transcriptome from RNA-seq reads. Nat. Biotechnol. 33 (3), 290–295. https://doi.org/10.1038/nbt.3122.

Pierce, R.H., Henry, M.S., Blum, P.C., Lyons, J., Cheng, Y.S., Yazzie, D., Zhou, Y., 2003. Brevetoxin concentrations in marine aerosol: Human exposure levels during a Karenia brevis harmful algal bloom. Bull. Environ. Contam. Toxicol. 70, 161–165. https://doi.org/10.1007/s00128-002-0170-y.

QuantSeq 3'mRNA-Seq Data Analysis | Lexogen [WWW Document], n.d. URL https://www.lexogen.com/quantseq-data-analysis/ (accessed 2.1.23).

Santander, M.V., Schiffer, J.M., Lee, C., Axson, J.L., Tauber, M.J., Prather, K.A., 2022. Factors controlling the transfer of biogenic organic species from seawater to sea spray aerosol. Sci. Rep. 12 (1), 1–11. https://doi.org/10.1038/s41598-022-07335-9.

Sloth Nielsen, L., Bilde, M., Laerke Sloth Nielsen, B., 2018. Exploring controlling factors for sea spray aerosol production: temperature, inorganic ions and organic surfactants. Chem. Phys. Meteorol. 72, 1–10. https://doi.org/10.1080/16000889.2020.1801305.

Tan, P.X., Thiyagarasaiyar, K., Tan, C.Y., Jeon, Y.J., Nadzir, M.S.M., Wu, Y.J., Low, L.E., Atanasov, A.G., Ming, L.C., Liew, K Bin, Goh, B.H., Yow, Y.Y., 2021. Algae-Derived Anti-Inflammatory Compounds against Particulate Matters-Induced Respiratory Diseases: A Systematic Review. Mar. Drugs 19, 317. https://doi.org/10.3390/MD19060317.

Team, R., 2014. R: A language and environment for statistical computing. MSOR connections.

Ullah, S., Sandqvist, S., Beck, O., 2015. Measurement of Lung Phosphatidylcholines in Exhaled Breath Particles by a Convenient Collection Procedure. Anal. Chem. 87, 11553–11560. https://doi.org/10.1021/ACS.ANALCHEM.5B03433/ASSET/IMAGES/MEDIUM/AC-2015-03433R_0005.GIF.

van Acker, E., de Rijcke, M., Asselman, J., Beck, I.M., Huysman, S., Vanhaecke, L., de Schamphelaere, K.A.C., Janssen, C.R., 2020. Aerosolizable Marine Phycotoxins and Human Health Effects. In Vitro Support for the Biogenics Hypothesis. Mar. Drugs 18, 46. https://doi.org/10.3390/MD18010046.

Van Acker, E., De Rijcke, M., Liu, Z., Asselman, J., De Schamphelaere, K.A.C., Vanhaecke, L., Janssen, C.R., 2021a. Sea Spray Aerosols Contain the Major Component of Human Lung Surfactant. Environ. Sci. Tech. 55, 15989–16000. https://doi.org/10.1021/ACS.EST.1C04075/SUPPL_FILE/ES1C04075_SI_001.PDF.

Van Acker, E., Huysman, S., De Rijcke, M., Asselman, J., De Schamphelaere, K.A.C., Vanhaecke, L., Janssen, C.R., 2021b. Phycotoxin-Enriched Sea Spray Aerosols: Methods, Mechanisms, and Human Exposure. Environ. Sci. Tech. 55, 6184–6196. https://doi.org/10.1021/acs.est.1c00995.

Van Meulebroek, L., Cameron, S., Plekhova, V., De Spiegeleer, M., Wijnant, K., Michels, N., De Henauw, S., Lapauw, B., Takats, Z., Vanhaecke, L., 2020. Rapid LA-REIMS and comprehensive UHPLC-HRMS for metabolic phenotyping of feces. Talanta 217, 121043. https://doi.org/10.1016/J.TALANTA.2020.121043.

Walter, L.O., Maioral, M.F., Silva, L.O., Speer, D.B., Campbell, S.C., Gallimore, W., Falkenberg, M.B., Santos-Silva, M.C., 2022. Involvement of the NF-κB and PI3K/Akt/mTOR pathways in cell death triggered by stypoldione, an o-quinone isolated from the brown algae Stypopodium zonale. Environ. Toxicol. 37, 1297–1309. https://doi.org/10.1002/TOX.23484.

Wheeler, B.W., White, M., Stahl-Timmins, W., Depledge, M.H., 2012. Does living by the coast improve health and wellbeing? Health Place 18, 1198–1201. https://doi.org/10.1016/J.HEALTHPLACE.2012.06.015.

White, M.P., Elliott, L.R., Grellier, J., Economou, T., Bell, S., Bratman, G.N., Cirach, M., Gascon, M., Lima, M.L., Lõhmus, M., Nieuwenhuijsen, M., Ojala, A., Roiko, A., Schultz, P.W., van den Bosch, M., Fleming, L.E., 2021. Associations between green/blue spaces and mental health across 18 countries. Sci. Rep. 11 (1), 1–12. https://doi.org/10.1038/s41598-021-87675-0.

Wickham, H., 2009. ggplot2 - Elegant Graphics for Data Analysis.

Yu, G., Wang, L.G., Han, Y., He, Q.Y., 2012. clusterProfiler: an R package for comparing biological themes among gene clusters. OMICS 16, 284–287. https://doi.org/10.1089/OMI.2011.0118.

Zhang, F., Du, J., 2017. How to Change the Chemical Composition of Sea Spray Aerosol via Marine Bloom. Chem. https://doi.org/10.1016/j.chempr.2017.04.019.

Zhao, C., Lin, G., Wu, D., Liu, D., You, L., Högger, P., Simal-Gandara, J., Wang, M., da Costa, J.G.M., Marunaka, Y., Daglia, M., Khan, H., Filosa, R., Wang, S., Xiao, J., 2020. The algal polysaccharide ulvan suppresses growth of hepatoma cells. Food Front. 1, 83–101. https://doi.org/10.1002/FFT2.13.